Ihor SHCHUR[1], Andrzej RUSEK[2], Oleksandr MAKARCHUK[3], Marek LIS[2]

National University "Lviv Polytechnic" (1,3),), Czestochowa University of Technology (2)

The Simulation Model of a Synchronous Machine with Permanent Magnets That Takes into Account Magnetic Saturation

Abstract. *The paper presents the methods of obtaining the parameters and characteristics of a synchronous machine with permanent magnets (PMSM) from the results of the previously conducted field electromagnetic study of a specific machine by the finite element method (FEM) in order to build a fairly accurate computer stimulation model of this machine. It shows that to model magnetic saturation, need to apply the resulting curves of magnetization by the flux of the armature reaction relative to the both d-axis and q-axis of the rotor, and this curves are invariant with respect to changes in the angle of orientation of the current vector relative to the rotor position. The results of work of simulation model are compared with the corresponding field modeling.*

Streszczenie. *Praca przedstawia metodę otrzymania parametrów i charakterystyk maszyny synchronicznej z magnesami trwałymi (PMSM) wykorzystując rezultaty elektromagnetycznych badań polowych konkretniej maszyny przeprowadzonych poprzednio metodą elementów skończonych (FEM) w celu stworzenia dokładnego modelu symulacyjnego tej maszyny. Pokazano, że dla modelowania nasycenia magnetycznego trzeba wykorzystać otrzymane krzywe magnesowania strumieniem reakcji twornika wzdłuż obuch d i q osi wirnika, ponadto te krzywe są inwariantne stosownie zmiany kąta orientacji wektora prądu stosunkowo pozycji wirnika. Wyniki symulacji komputerowej PMSM porównano z odpowiednim modelowaniem polowym. (**Model symulacyjny silnika synchronicznego z magnesami trwałymi uwzględniający nasycenie magnetyczne)***

Keywords: PMSM, magnetic saturation, FEM, simulation model.
Słowa kluczowe: PMSM, nasycenie magnetyczne, FEM, model symulacyjny.

Introduction

Synchronous machines with permanent magnets (PMSM) and electronic switching, due to their good controlling in a wide range of speed, high energy efficiency, and durability, have been put to increasingly more uses in recent years, including in electric drives of machine tools, robots, electric vehicles, etc. [1,2]. A large number of vector control systems for PMSM have been developed, which are usually based on a mathematical model of PMSM with constant parameters [2,3]. The same model is used to build a virtual PMSM in the library SimPowerSystem in Matlab/Simulink. However, the high value of power density in PMSM and its high overload capacity cause the machine to work with the deep saturation of magnetic paths. The manifestations of this phenomenon change the parameters and characteristics of the machine as a control object, which leads to the worsening in the work of the control algorithms. In order to carry out simulation studies of PMSM control systems in their sensitivity to the parametric changes of the object, fast computer models of machines, which take into account magnetic saturation, are required. There is a series of papers on the mathematical description of PMSM taking into account the saturation [4-6]. Precise computer models of PMSM that take saturation into account can be obtained from the description of the electromagnetic fields in the distributed parameters using the finite element method (FEM) [1]. However, high intensity and duration of computer field studies do not permit their use in the computer modeling of control systems. This study aims at developing precise mathematical and very fast computer simulation models of PMSM, which are based on the results of previously conducted field studies, in order to apply these models to create a robust system of electric drives.

The mathematical description of PMSM

The most effective is the mathematical model of PMSM in a rectangular reference frame dq linked with the rotor, when the d axis is oriented along the vector of the flux of permanent magnets (PM) [2,3]:

$$u_d = R_s i_d + \frac{\mathrm{d}}{\mathrm{d}t}\psi_d - \omega\psi_q$$

$$u_q = R_s i_q + \frac{\mathrm{d}}{\mathrm{d}t}\psi_q + \omega\psi_d \tag{1}$$

where u, i, ψ are the voltage, the current, and the flux linkage respectively, R_s is the resistance of phase winding of the stator, $\omega = p_b\omega_r$ is the radiant frequency of EMF, p_b is the number of pairs of poles, and ω_r is the angular speed of PMSM.

Projections of flux linkage on the *dq* axis are

$$\psi_d = \psi_{id} + \psi_m = L_d i_d + \psi_m$$

$$\psi_q = \psi_{iq} = L_q i_q \tag{2}$$

where ψ_i is the flux linkage of armature reaction, L is the inductance, and ψ_m is the flux linkage from the PM.

One of the methods of PMSM vector control, which is most often used, especially for motors with surface mounting PM – SPMSM, is maintaining $i_d = 0$. For machines with PM embedded in rotor iron – IPMSM, as well as for all the PMSM that work with the field weakening, $i_d < 0$. From (2) it is clear that in all these cases, the component of flux linkage ψ_d does not increase with increasing current component i_d. That is why the magnetic saturation along the axis d is practically absent. At the same time, the magnetic saturation along the axis q takes place, which is expressed by the non-linear dependence $\psi_{iq}(i_q)$. In general, we take into account also the possible non-linear dependence $\psi_{id}(i_d)$. The time derivatives of both components of flux linkage looks like

$$\frac{\mathrm{d}}{\mathrm{d}t}\psi_d(i_d) = \frac{\mathrm{d}\psi_{id}(i_d)}{\mathrm{d}i_d}\cdot\frac{\mathrm{d}i_d}{\mathrm{d}t} = \hat{L}_d(i_d)\frac{\mathrm{d}}{\mathrm{d}t}i_d$$

$$\frac{\mathrm{d}}{\mathrm{d}t}\psi_q(i_q) = \frac{\mathrm{d}\psi_{iq}(i_q)}{\mathrm{d}i_q}\cdot\frac{\mathrm{d}i_q}{\mathrm{d}t} = \hat{L}_q(i_q)\frac{\mathrm{d}}{\mathrm{d}t}i_q \tag{3}$$

where $\hat{L}_d(i_d)$ and $\hat{L}_q(i_q)$ are the dynamic inductances.

Substituting (2) and (3) in (1), we obtain the following system of nonlinear differential equations describing the electrical balance in PMSM:

$$u_d = R_s i_d + \underbrace{\hat{L}_d(i_d)\frac{\mathrm{d}}{\mathrm{d}t} i_d}_{1} - \underbrace{\omega \psi_{iq}(i_q)}_{2}$$

$$u_q = R_s i_q + \underbrace{\hat{L}_q(i_q)\frac{\mathrm{d}}{\mathrm{d}t} i_q}_{1} + \underbrace{\omega \psi_{id}(i_d)}_{2} + \underbrace{\omega \psi_m}_{3} \quad (4)$$

In (4) terms 1 express the EMF of self-induction, 2 express the EMF caused by armature reaction, and 3 - rotation EMF.

The electromagnetic torque of the motor has the form

$$T = \frac{3}{2} p_b \left[\psi_d(i_d)\, i_q - \psi_q(i_q)\, i_d\right] \quad (5)$$

The complete mathematical model of PMSM must also include the model of the mechanical part of the drive, for example, of a one mass part:

$$J\frac{d}{dt}\omega_r + b\omega_r = T - T_l \quad (6)$$

where J is the total moment of inertia of the drive system, given to the motor shaft, b is the coefficient of viscous friction, and T_l is the torque of static load.

The obtained mathematical model, that takes magnetic saturation into account, contains variables non linearly dependent from current $\psi_{id}(i_d)$, $\psi_{iq}(i_q)$ and $\hat{L}_d(i_d)$, $\hat{L}_q(i_q)$. We suggest determining these dependences on the basis of the results of field study of PMSM.

The results of field studies of experimental PMSM

For this study, we selected a PMSM with four poles, commercially produced by BOBRME "Komel" (Poland), IPMSg132 S4 PMSM with the following rated parameters: power 4 kW, voltage 400 V, the speed of 1500 rev/min. PM are buried in the rotor as shown in Figure 1.

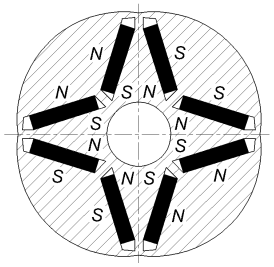

Fig. 1. The design of the rotor in the studied PMSM

Research was carried out by calculation. The calculation of a two-dimensional magnetic field for given boundary conditions and density currents in conductive areas was done by FEM using specialized software ANSYS [7].

In the first stage, the dependences of induction of the PM magnetic field in the air gap and its flux linkage with the phase windings in the absence of phase currents are investigated. The radial B_r and tangential B_τ components of the vector of induction of the magnetic field in the air gap, obtained as the result of such calculation, depending on the angular coordinate γ [º el.] are shown in Figure 2. For a quantitative estimation of the obtained results, the tabulated functions $B_r(\gamma)$ are decomposed in a Fourier series. 20 harmonics were evaluated, but the amplitudes of the harmonics of "tooth" orders were not taken into account.

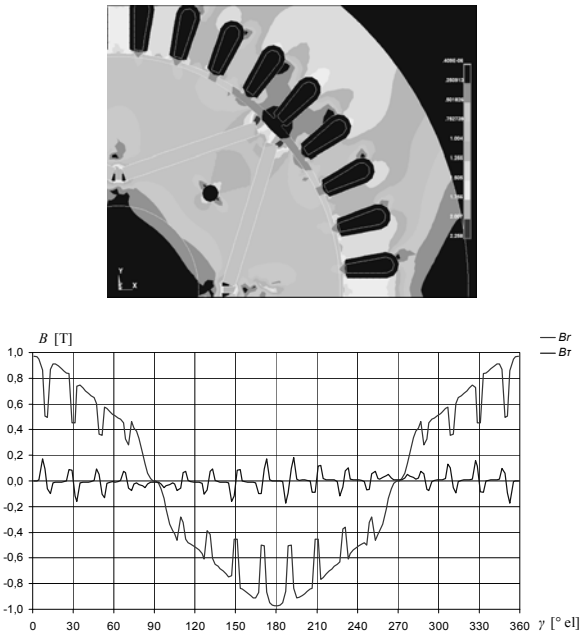

Fig. 2. The field of PM magnetic induction and angular dependences of its radial *Br* and tangential *Bτ* components

The harmonics of flux linkages of the PM field with phase armature windings, calculated on the field model of the studied PMSM as a function of the angle of rotor rotation $\boldsymbol{\psi}_{mabc}(\gamma) = \left[\psi_{ma}(\gamma) \quad \psi_{mb}(\gamma) \quad \psi_{mc}(\gamma)\right]^{\mathrm{T}}$, shown in Table 1. These spatial harmonics are used for modeling the rotation EMF of machines in *abc* coordinates (term 3 in equation (4)):

$$\psi_{mk}(\gamma) = \sum_i \left\{\psi_{m.\sin i} \sin\left[i\delta_k(\gamma)\right] + \psi_{m.\cos i} \sin\left[i\delta_k(\gamma)\right]\right\} \quad (7)$$

where $\psi_{m.\sin i}$ and $\psi_{m.\cos i}$ are respectively the sin and cos components of the *i*-th field harmonic of PM flux linkage from Table 1, $k = a, b, c$, $\delta_k(\gamma) = \gamma + \Delta\varphi_k$, $\Delta\varphi_a = 0$, $\Delta\varphi_b = -2\pi/3$, $\Delta\varphi_c = 2\pi/3$.

Table 1. Parameters of the harmonics of flux linkage of the rotor PM with armature windings

No of harmonic, i	$\psi_{m.\sin i}$, Wb	$\psi_{m.\cos i}$, Wb
1	$-1.040\cdot10^{-1}$	$-5.910\cdot10^{-1}$
2	$8.515\cdot10^{-7}$	$3.357\cdot10^{-6}$
3	$3.700\cdot10^{-3}$	$6.392\cdot10^{-3}$
4	$-8.111\cdot10^{-6}$	$3.134\cdot10^{-5}$
5	$-1.401\cdot10^{-3}$	$-1.175\cdot10^{-3}$
6	$8.482\cdot10^{-6}$	$4.360\cdot10^{-5}$
7	$-4.772\cdot10^{-4}$	$-1.723\cdot10^{-4}$
8	$-4.570\cdot10^{-6}$	$-6.464\cdot10^{-6}$
9	$1.967\cdot10^{-4}$	$2.596\cdot10^{-6}$

As seen from the obtained results, the corresponding profiling of the surface of the rotor core that provides uneven working air gap enables field distribution close to sinusoidal.

In the second stage, the magnetic field of the machine powered from the current source was investigated. We selected three operating values of the armature current – 9,

18 and 27 A as well as different outstripping angles of the current vector relative to the first harmonic of the EMF rotation vector caused by PM, – δ = -30, -10 and +20º el. The form and value of the electromagnetic torque were reproduced while taking comprehensively into account all the factors that occur in the real conditions of machine work and in their interrelationship, namely: the armature reaction given the saturation of the magnetic core; real harmonic structure of the magnetic intensity force of armature winding taking into account the harmonics of tooth orders; magnetic anisotropy of inductor poles in two spatial coordinates; reluctance torques caused by power interaction of PM with structural elements of the magnetic core.

Figure 3 shows the time dependences of given phase currents and obtained basic coordinates of drive T, ω_r and γ_r, when you start the machine under load and with the discrete change in set values of the armature current at the outstripping angle δ = -10º el.

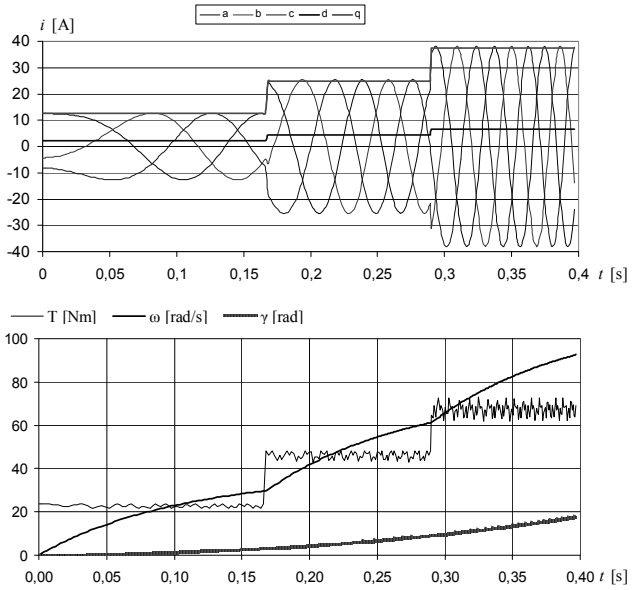

Fig. 3. Time dependences of phase currents i, electromagnetic torque T, angular speed ω_r and angle of rotor rotation γ_r during machine startup, obtained on the field model of PMSM

The moment of inertia of the rotating parts was J = 0.0646 kg·m^2. The static load torque was formed in proportion to the rotation speed according to the expression

$$T_l = -T_{ln}\,\omega_r / \omega_{rn}$$

where ω_{rn} = 41.9 rad/s is the rated angular speed and T_{ln} =25.5 N·m is the rated load torque.

Figure 4 shows the dependences of phase complete flux linkages on the angle of rotor rotation, obtained for this case of PMSM acceleration.

Methods of modeling magnetic saturation

Machine options necessary for modeling magnetic saturation can be obtained from computational experiments of the field study of a specific PMSM in accordance with the following procedure.

1. On the basis of the obtained angular dependences of the vector components of flux linkage $\boldsymbol{\psi}_{mabc}(\gamma)$ caused by the action of PM, and the vector components of complete flux linkage of PMSM $\boldsymbol{\psi}_{\Sigma abc\,j}\left[\mathbf{i}_{abc\,j}(\gamma),\gamma\right]$ for a specific outstripping angle and some j = 1,…,n values of the armature current, the values of the vector components of flux linkage of the armature reaction in the first approximation can be found as the difference between the values of the respective components of these vectors:

$$\boldsymbol{\psi}_{i abc\,j}\left[\mathbf{i}_{abc\,j}(\gamma),\gamma\right] = \boldsymbol{\psi}_{\Sigma abc\,j}\left[\mathbf{i}_{abc\,j}(\gamma),\gamma\right] - \boldsymbol{\psi}_{m abc}(\gamma) \tag{8}$$

2. The obtained components of the vector of flux linkage of the armature reaction and the corresponding components of the vector of current should be converted to a reference frame dq:

$$\boldsymbol{\psi}_{i dq\,j}\left(\mathbf{i}_{dq\,j}\right) = \left[\psi_{i d\,j}\left(i_{d\,j}\right) \quad \psi_{i q\,j}\left(i_{q\,j}\right)\right]^{\mathrm{T}} \tag{9}$$

3. From the vectors of flux linkage for the smallest current value (without saturation) $\boldsymbol{\psi}_{i abc\,1}\left[\mathbf{i}_{abc\,1}(\gamma),\gamma\right]$ and $\boldsymbol{\psi}_{i dq\,1}\left(\mathbf{i}_{dq\,1}\right)$ the inductances can be found according to the method described in [10]: leakage L_σ, magnetization at d axis L_d, and the initial (unsaturated) magnetization at q axis $L_{q\,start}$.

4. The dependence $\psi_{i d\,j}\left(i_{d\,j}\right)$ and $\psi_{i q\,j}\left(i_{q\,j}\right)$, obtained in step 2, should be approximated by the function [11]

$$\psi(i) = a_1 \arctan(a_2 i) + a_3 i \tag{10}$$

where a_1, a_2, a_3 are the coefficients of approximation.

Then the dependence of the dynamic inductance on the current is equal

$$\hat{L}(i) = \frac{a_1 a_2}{1 + a_2^2 i^2} + a_3 \tag{11}$$

Steps 1-4 are repeated for other values of the outstripping angle of the current vector relative to the vector of rotation EMF.

Figure 4 shows the obtained angular dependences of phase flux linkages of the armature reaction and their projections in rotating *dq* coordinates during acceleration of PMSM for outstripping angle δ = -10º el. All factors taking into account in the field model (tooth structure of the armature, the real distribution of the armature winding, magnetic core saturation) causes non-sinusoidal phase linkages and corresponding ripple of their *dq* projections.

Figure 5 shows the dependences $\psi_{i d\,j}\left(i_{d\,j}\right)$, $\psi_{i q\,j}\left(i_{q\,j}\right)$, obtained according to the described methods, at three values of the studied outstripping angle.

As seen from the results, there are good agreement between them; therefore, regardless of the orientation of the current vector, the obtained nonlinear curves of armature reaction and correspondent dynamic inductances, using (10) and (11), should be approximated by the following dependencies:

$$\begin{aligned}
\psi_{i d}\left(i_d\right) &= 0.147 \arctan(0.09\, i_d) - 0.028 \\
\psi_{i q}\left(i_q\right) &= -0.286 + 0.0185\, i_q - 9.25 \cdot 10^{-5} i_q^2 \\
\hat{L}_d\left(i_d\right) &= \frac{0.0132}{1 + 0.0081 i_d^2} \\
\hat{L}_q\left(i_q\right) &= 0.0185 - 18.5 \cdot 10^{-5} i_q
\end{aligned} \tag{12}$$

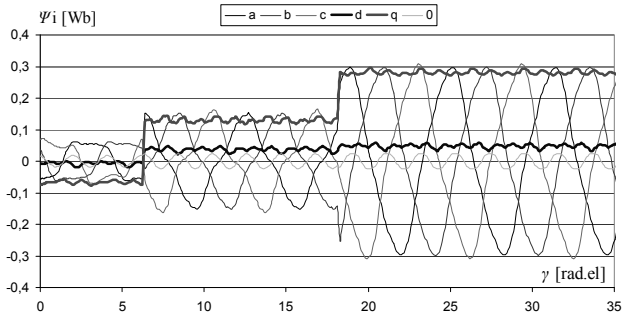

Fig. 4. Dependences of phase flux linkages of the armature reaction of PMSM, as well as their projections in rotating *dq* reference frame, on the angle of rotor rotation during machine acceleration

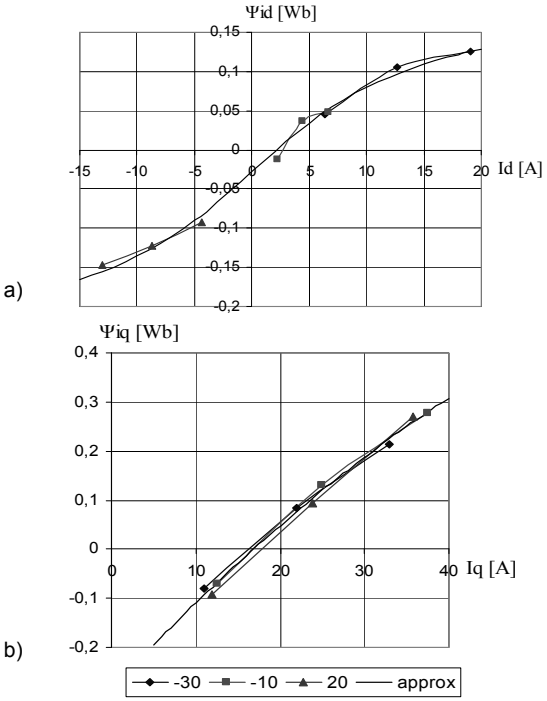

Fig. 5. The obtained dependences of flux linkage of the armature reaction on the current along *d* axis (a) and *q* axis (b) at different angles of orientation of the armature current vector relative to the rotor

Computer simulation model of RMSM with taking saturation into account

The computer simulation model of PMSM is constructed in the software Matlab/Simulink based on the expressions (4) - (6). To approximate reality as much as possible and for easy combination with other models from the Simulink library, PMSM is modeled as a virtual three-phase one. In the dq reference frame, only those elements are modeled which reflect the different nature of processes in the direction of these axes (components 1 and 2 in equation (4)). The model uses the subsystems, which are utilized to calculate the flux linkage caused by PM, total EMF, and electromagnetic torque of PMSM. PM flux is forming in the phase coordinates abc, and in harmonic subsystems equation (7) is implemented. Total EMF and electromagnetic torque is described in *dq* reference frame with the use of the obtained equations (12) and subsystems of coordinate transformation

Figure 6 shows the time dependences of the basic coordinates of PMSM at machine acceleration, which were obtained with using the developed stimulation model of PMSM for the same conditions as in the field study (Fig. 3).

The results in both cases showed very good agreement, but the computing time differed radically: 16 hours in the field study and 12 seconds in the computer simulation.

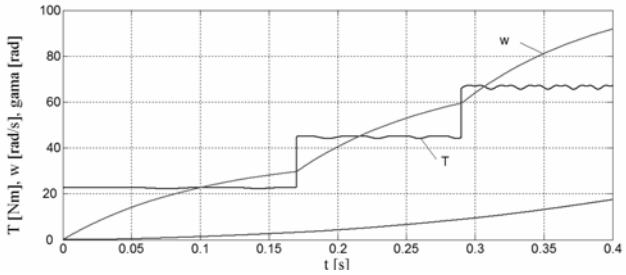

Fig. 6. The time dependences of electromagnetic torque T, angular velocity ω_r and angle γ_r of rotor rotation during the startup of the machine, obtained in simulation of PMSM

Conclusion

The results of field modeling (FEM) of the electromagnetic processes in PMSM, which are highly reliable, serve as a good basis for obtaining sufficiently accurate, yet simple, stimulation computer models of machines, which take into account the spatial field harmonics and the phenomenon of the saturation of magnetic paths. Such models, because of their speed, can be successfully used in developing the highly dynamic and robust control systems of electric drives based on PMSM.

REFERENCES

[1] Gieras J.F., Wing M., *Permanent Magnet Motor Technology. Design and Applications*, Marcel Dekker, NY, (2002)

[2] Krause P.C., Wasynczuk O., Sudhoff S.D., *Analysis of Electric Machinery and Drive Systems*, IEEE PRESS, Wiley Interscience, (2002)

[3] Sieklucki G., *Automatyka Napędu*, Wydawnictwa AGH, Kraków, (2009)

[4] Corzine K.A., Kuhn B.T., Sudhoff S.D., Hegner H.J., An improved for incorporating magnetic saturation in the q-d synchronous machine model, *IEEE Trans. Energy Convers.*, 13 (1998), No. 3, 270-275

[5] Levi E., State-space d-q axis models of saturated salient pole synchronous machines, *IEE Proc.-Electr. Power Appl.* 145 (1998), No. 3, 206-216

[6] Prokop J., Nowe równania modeli obwodowych maszyn elektrycznych z magnesami trwałymi, *Przegląd Elektrotechniczny*, 86 (2010), nr 2, 1-8

[7] Shchur I., Rusek A., Makarchuk O., Modelowanie symulacyjno-komputerowe silnika synchronicznego z magnesami trwałymi na podstawie wyników badań polowych, *Maszyny elektryczne. Zeszyty problemowe*, 96 (2012), nr 3, 189-195

[8] Keyhani A., Tsai H., Igspice simulation of induction machines with saturable inductances, *IEEE Trans. Energy Convers.*, 4 (1989), No. 1, 118-125

***Authors**: prof. dr hab. inż. Ihor Shchur, Politechnika Lwowska, Instytut Energetyki i Układów Sterowania, ul. Bandery 12, 79013 Lwów, Ukraina, E-mail: i_shchur@meta.ua, dr hab. inż. Andrzej Rusek, Politechnika Częstochowska, Wydział Elektryczny, Instytut Elektrotechniki Przemysłowej, E-mail: rusek@el.pcz.czest.pl, dr inż. Oleksandr Makarchuk, Politechnika Lwowska, Instytut Energetyki i Układów Sterowania, ul. Bandery 12, 79013 Lwów, Ukraina, E-mail: makar_lp@rambler.ru, dr inż. Marek Lis, Politechnika Częstochowska, Wydział Elektryczny, Instytut Elektrotechniki Przemysłowej, E-mail: lism@el.pcz.czest.pl,*